Realization of 2D pressure sensor using germanium photonic crystal waveguide via FDTD method

C. S. MISHRA[1], G. PALAI[2,*], R. N. SATPATHY[2], P. SARKAR[3]
[1]*Department of ECE, Gandhi Institute for Technological Advancement (GITA), Bhubaneswar, India*
[2]*Sri Sri University, Cuttack, Odisha, 754006, India*
[3]*JIS College of Engineering, West Bengal, India*

In this research paper, Germanium based L-shape photonic crystal structure is used to realise a pressure sensor pertaining to the amount of pressure ranging from 0 gigapascal to 10 gigapascal. Further, the electric distribution field in the 'L' shape defect (15×15) is computed at the incident signal of 1550 nm (laser source), where the radius of the germanium rods varies from 410 nm to 440 nm at the same pressure range and lattice spacing remains 900 nm. Further, the output power is thoroughly discussed with respect to the peak electric field of output simulation. Here, the principle of sensing mechanism relies on the electric field distribution pertaining to the different pressures (up to 10 GPa). The radius (r=0.42a) of the rod outlet depends on the lattice constant (a). The simulation is done for all variations of pressure and radius of the rod, where the finite difference time method is applied to obtain electric field distribution. The output power result shows mixed linear as well as nonlinear behavior with respect to the increment of radius at the applied pressure range. This research paper is applicable for pressure sensing with respect to the 2D photonic crystal (Ge).

(Received December 1, 2023; accepted June 3, 2024)

Keywords: Photonic crystal fiber, Pressure, 2D photonic crystal, FDTD, Pressure, Electric field distribution

1. Introduction

In the late 19th century, Yablonovitch [1] and John [2] demonstrated the localization of light in disordered dielectric constant substances in contrast to the photonic crystals (PCs), which are well known for suppressed arbitrary emission of light. Periodical iteration of the PCs' refractive index contributes to strengthening the Bloch waves with respect to forming photonic bandgaps (PBGs). Transmission is limited within a certain frequency range after an incident of light to PBG material. Complete PBGs can only be achieved for three-dimensional (3D) PCs but pose many fabrication and experimentation challenges. However, fabrications of 2D PCs are much more accessible and can be integrated by using periodically spaced rods in air or holes throughout the substrate [3-4]. The three types of photonic crystals have been operating in the manufacturing industry to improve quality and competitiveness for society's benefit since 1987. This photonic technology is available in a variety of communication applications like temperature sensors, displacement sensors, nonlinear devices, pressure sensors, etc. [5-10]. Several recent publications on the application of photonic crystals have been published. For example, a label-free pressure sensor is designed with regard to the refractive index [11]. The high sensitivity is found in two dimensional photonic based sensors [12]. The sensing properties of 2D photonic crystals are investigated from an applied pressure 0 GPa to 7 GPa [13]. The amount of pressure and wavelength of resonance of the two-dimensional photonic crystal sensor shows the fine linear ship [14]. The colour variation occurred due to a silicon nanowire modulation, deflection angle, and pitch in all-optical pressure sensors [15]. The application of photonic crystal has been observed in biosensing (proteins, avidins, BSA, DNA, etc.) [16-19], dengue virus detection [20] and chemical sensing [21-24]. The power efficiency of the 2D photonic crystal is calculated for sensing applications [25]. The nano-ring resonant based photonic pressure sensor is developed due to optimize the resonance wavelength shift [26]. The sensitivity of the pressure sensor is developed on a GaAs membrane [27]. The demonstration of high sensitivity is found in the range of microscale pressure sensors [28]. The 2-dimensional PhC-based micro-optical pressure sensor has been considered as a Si substrate [29]. Line defect photonic crystal waveguide is narrated on a hanging silicon substrate [30]. Analysis of pressure sensors is investigated in terms of the refractive index of the material [31]. The high-quality factor and sensitivity of a pressure sensor through a two-dimensional photonic crystal is thoroughly investigated [32-34]. The various applications of 2D PC structure within the field of photonics include optical encoders, sensors, logic gates, optical switches, and photonic crystal-based devices, showcasing the diverse research in this area [49-55]. Although 2D crystals are beginning to encounter commercial applications, our focus is on a two-dimensional photonic crystal for application of pressure sensors utilizing germanium (Ge) material. In this article; we also design the germanium-based two-dimensional pressure sensor with the variation in the radius of rods. The projected photonic based pressure sensor consists of an L-shaped waveguide with a square lattice of air gaps. The sensor characteristics are evaluated, where the finite difference time domain approaches are used to solve this problem. The present paper bestows the germanium-based 2D photonic pressure sensor due to the application in

the nanotechnology industry.

2. Design and analysis of germanium PCW

In the current investigation, a 2D square lattice germanium photonic crystal waveguide is designed to measure output power with respect to structure parameters such as radius and lattice spacing at applied pressure. The incident signal is a wavelength of 1550 nm. The structure comprises 15×15 germanium photonic crystal poles placed together round germanium substrate. Imperfection as an L-shape is deliberately made along the proposed structure's focal point to allow a 90 degree bend, which is graphically illustrated in Fig. 1. The 11th germanium rod is removed because of the defect.

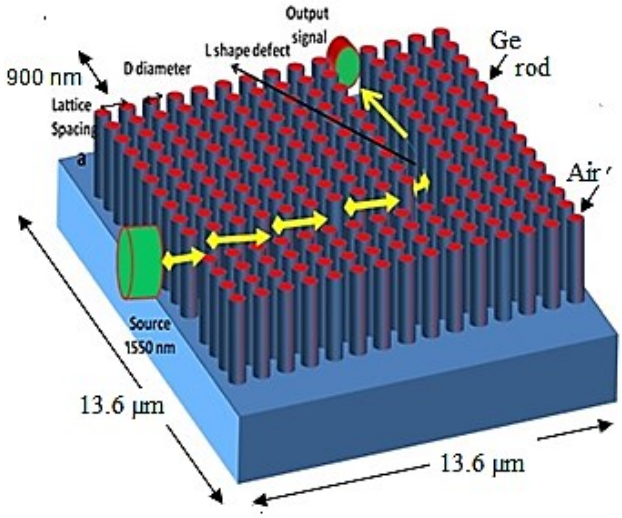

Fig. 1. L defect based photonic crystal waveguide at different pressures in GPa (color online)

Each side length of the proposed structure is viewed as 13.6µm, while the permittivity of foundation round about bars is viewed as 1.0 (the permittivity of air is 1) [27]. The wavelength of signal 1550 nm (laser source) has impinged on the defect region of a germanium based two dimensional (2D) photonic crystal, where the pressure ranges from 0 to 10 GPa is applied uniformly to the aforementioned proposed configuration. The light propagates through the L shaped defect waveguide, which is illustrated in Fig. 1. At the output end of the structure (yellow arrow mark inside), the peak electric field is measured. The simulation (Mat Lab software) has been conducted using the Finite-Difference Time-Domain (FDTD) method across a range of germanium material rod radii with respect to a wide range of pressures (0-10 GPa), specifically from 0.41 µm to 0.44 µm, encompassing values of 0.41 µm, 0.42 µm, 0.43 µm, and 0.44 µm. But the simulation curve of radius 0.41 µm at 0 (pressure) GPa is shown in Fig2 2, where the peak electric field is 0.5613 V/µm. In FDTD, space and time are discretized into a grid. The size of the grid cells in space and time, often denoted by Δx and Δt, respectively, which determines the spatial and temporal resolution of the simulation. Smaller grid cells result in higher resolution but require more computational resources. In this research, we use the 900 nm and 5.4×10^{-16} second as space and time intervals. As far as the computational domain is concerned, here the electromagnetic fields are simulated using Perfectly Matched Layers (boundary), to absorb outgoing waves and prevent reflections from the edges of the domain.

The peak electric field distribution of the photonic structure's output with different pressures has been reported with respect to the different radii in Table 1.

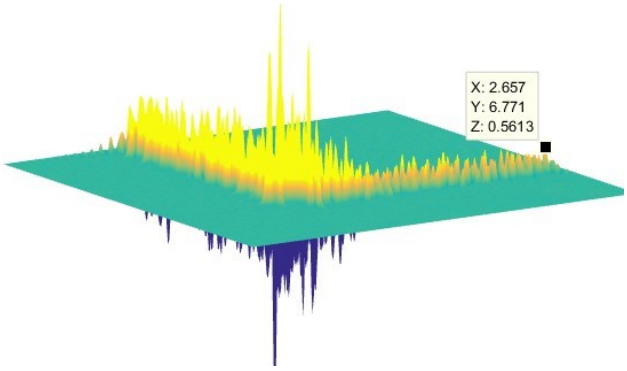

Fig. 2. Electric field distribution of radius 0.41 µm at applied pressure 0 GPa (color online)

Table 1. Output electric field distribution with respect to the radius and pressure (lattice spacing 0.9µm)

Pressure in GPa	0	1	2	3	4	5	6	7	8	9	10
Output E_peak (V/µm), R(0.41µm)	0.5613	0.5297	0.4584	0.3864	0.3129	0.3376	0.3594	0.3782	0.3773	0.3788	0.3813
Output E_peak (V/µm) R(0.42µm)	0.565	0.5297	0.4584	0.5167	0.526	0.5709	0.621	0.6304	0.6597	0.6517	0.6496
Output E_peak (V/µm) R(0.43µm)	0.541	0.5654	0.5971	0.6195	0.6365	0.6486	0.6808	0.685	0.7257	0.7309	0.7502
Output E_peak (V/µm) R(0.44µm)	0.8804	0.8884	0.8725	0.8902	0.9309	0.9445	0.9639	0.9688	0.9716	0.9645	0.9621

The output power is computed by using Table 1 and power eq. 1, which is given below [35-36]

$$\text{Power}=0.5\epsilon_0 cAnE^2 \quad (1)$$

where E, A, n, c and $\epsilon_0$are the electric field, area of structure, refractive index of material and permittivity of vacuum respectively

An L-shaped imperfection at the focal point of a silicon two-dimensional photonic crystal offers significant advantages, notably in facilitating a 90-degree bend in the propagation of light. This deliberate deviation from the regular lattice structure acts as a guide, directing light waves along a predetermined path. By strategically placing the imperfection, precise control over the directionality of the bend is achieved, which enables the design of compact optical circuits and devices with enhanced functionality. Moreover, the tailored imperfection minimizes scattering and absorption losses, resulting in improved overall efficiency of the photonic device. This approach not only enables the manipulation of light with precision but also opens avenues for the development of advanced integrated photonics systems capable of performing complex optical tasks efficiently.

3. Result and discussion

The amount of power produced in the aforementioned two-dimensional germanium based photonic structure can be calculated using eq. 1. The output results corresponding to everyone's selected radius are illustrated in Fig. 3.

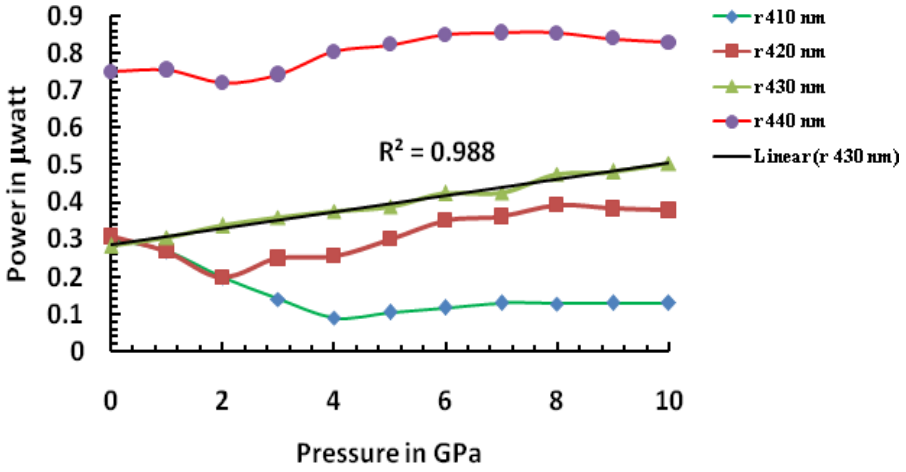

Fig. 3. Pressure and output power of PCW (15x15) with L shape defect with different radius ranges (color online)

Fig. 3 shows that pressure in GPa has been taken on the x-axis, and power has been taken on the y-axis in µwatts. The nature of the curve depicts that output power increases approximately linearly with respect to an increment of applied pressure. However, the output power for radius 430 nm shows a good linear ship approximately because of trend line value is 99%. Further, high power in microwatt seems at r=440 nm, which shows good for pressure sensor application at this radius. Photonic pressure sensing leverages the interaction of light with materials to detect and measure pressure-induced changes. High power levels play a crucial role in enhancing the performance of these sensors by inducing nonlinear behaviour in the sensing material. This nonlinear behaviour leads to increased sensitivity, improved signal-to-noise ratio (SNR), and an expanded dynamic range, making the sensor more capable of detecting subtle pressure variations. Several research studies have explored the benefits of high-power photonic pressure sensors using various configurations and materials. For instance, Yu and Fan (2013) demonstrated the efficiency of small-footprint optical pressure sensors based on photonic crystal nanobeams, highlighting the potential for compact and sensitive sensing devices [44].

Kuiri et al. (2024) demonstrate the potential of nano-engineered photonic sensors in various applications requiring precise refractive index measurements, highlighting its relevance in fields such as biochemical sensing and environmental monitoring. [45]. in another study, Xia et al. (2020) proposed an integrated photonic crystal cavity-optomechanical sensor, illustrating the integration of photonic and mechanical elements to achieve high sensitivity in pressure measurements [46]. Furthermore, Zhang et al. (2016) and Li and Huang (2018) explored the use of photonic crystal nanobeam resonators for high-sensitivity pressure sensing applications. These studies highlighted the significance of design considerations and fabrication techniques in achieving optimal sensor performance [47-48].

Overall, these references provide valuable insights into the design, fabrication, and applications of high-power, two-dimensional photonic pressure sensors. By leveraging nonlinear effects and optimizing sensor configurations, researchers aim to develop sensitive, compact, and reliable sensing devices for a wide range of applications, including biomedical diagnostics, environmental monitoring, and industrial process control.

4. Comparison among the referenced papers with respect to current paper

Ayyanar et al. (2016) [37]: Ayyanar and colleagues developed a hydrostatic pressure sensor using high birefringence photonic crystal fibers. Their work focused on utilizing the unique properties of photonic crystal fibers to achieve pressure sensing capabilities. While their sensor operates based on hydrostatic pressure, the current paper proposes a pressure sensor using Germanium-based L-shape photonic crystal structures. Ayyanar et al.'s sensor relies on birefringence effects, while the current paper utilizes the electric field distribution in photonic crystal structures for pressure sensing.

Turduev et al. (2017) [38]: Turduev and his team designed a mid-infrared T-shaped photonic crystal waveguide for optical refractive index sensing. Their work targets sensing applications related to refractive index changes in the mid-infrared spectrum. In contrast, the current paper focuses on pressure sensing using Germanium-based L-shape photonic crystal structures operating at a specific incident wavelength of 1550 nm. While Turduev et al.'s work addresses refractive index sensing, the current paper addresses pressure sensing, demonstrating the versatility of photonic crystal structures in different sensing applications.

Dinodiya et al. (2022) [39]: The current paper's results demonstrate an improvement in the pressure sensing range, covering 0 GPa to 10 GPa, which is a wider range compared to the 5 GPa range reported by Dinodiya et al. Additionally, the discussion on electric field distribution at a specific incident signal wavelength of 1550 nm provides deeper insights into the sensing mechanism.

Panoiu et al. (2022) [40]: While Panoiu et al. focused on crucial parameters, such as pulse group velocity, dispersion coefficients, and the waveguide nonlinear coefficient. Additionally, slow-light modes exhibit stronger linear and nonlinear effects, with a more substantial enhancement observed in the nonlinear effects. The current paper not only employs FDTD but also extends the analysis to discuss the mixed linear and nonlinear behavior of output power with respect to varying pressure and air hole radius. This comprehensive analysis adds depth to the understanding of the photonic crystal's behavior under pressure.

Morini et al. (2018) [41]: Morini et al. investigated electric field distribution in waveguide but did not specifically focus on pressure sensing applications. In contrast, the current paper not only analyzes the electric field distribution but also establishes its correlation with pressure variations, thereby directly addressing the pressure sensing aspect.

Mishra et al. (2022) [7]: The L shaped Photonic Crystal waveguide analysis reported for terahertz communication, the current paper's discussion on the nonlinear behavior of output power concerning pressure and germanium rod radius variations. This provides a more comprehensive understanding of the photonic crystal's response to varying pressure conditions.

Singh et al. (2017) [43]: Singh et al. investigated the power splitter based on photonic crystal waveguide but did not explore the pressure sensing range comprehensively. The current paper not only optimizes the germanium rod radius but also provides a thorough analysis of pressure sensing performance across a wide pressure range, thus offering a more holistic approach to enhancing pressure sensing capabilities. The comparison in Table 2 summarizes various pressure sensing techniques utilizing different sensor types, materials, sensing principles and applications.

Table 2. Comparison of 2D L-shape photonic crystal structures (pressure sensing and power amplification)

Reference	Sensor Type	Material Used	Sensing Principle	Application
Ayyanar et al. (2016) [37]	Photonic crystal Fiber optic	Silica	Birefringence	Hydrostatic pressure
Turduev et al. (2017) [38]	Photonic crystal Waveguide T-shaped	Silicon	Refractive index change	Refractive index sensing
Dinodiya et al. (2022) [39]	Photonic crystal Waveguide	Si and GaAs	shifting of central wavelength	Pressure sensing
Zouache et al. (2017) [32]	Photonic crystal Waveguide	Germanium	Finite Difference Time Domain plane wave expansion method	Pressure sensing
Morini et al. (2018) [41]	Photonic crystal Waveguide	Germanium	Electric field distribution	telecom and datacom
Mishra et al. (2022) [42]	Photonic crystal Waveguide	InAs and ZnO	plane wave expansion (PWE)	Pressure sensing
Singh et al. (2017) [43]	Photonic crystal Waveguide	Silicon	Finite-Difference Time Domain (FDTD)	multi-arm power splitter
Mishra et al. (2019) [7]	L shaped photonic crystal waveguide	Silicon	Finite Difference Time Domain	Terahertz (THz) communication

Reference	Sensor Type	Material Used	Sensing Principle	Application
Shaiket et al. (2016) [56]	T-shaped waveguide	Silicon	plane-wave expansion and finite difference time domain methods	High-speed broadband optical communication and networks.
Shaik et al. (2016) [57]	T-shaped waveguide	Silicon	Power Amplification PWE and FDTD	High speed broadband optical communication systems and networks
Askarian et al. (2023) [58]	Photonic crystal Waveguide	Silicon	finite difference time domain (FDTD)	Enhanced power amplification in optical systems
Bhavana et al. (2023) [59]	T-shaped waveguide	GaAs	Electric field distribution(FDTD)	optical interconnect in the light wave circuit, Enhanced power amplification in optical systems
T Li et al. (2014) [60]	L-shaped microcantilever	Silicon	Finite element method and finite difference time-domain method	optical nanomechanical sensor
T Kim et al. (2019) [61]	Photonic crystal Waveguide	Silicon	Electric field distribution	C-band coherent optical receiver
Latha et al. (2019) [62]	Y-Shaped Photonic Crystal Waveguide:	Gallium Arsenide (GaAs)	Finite difference time-domain method	ENCODER
This paper (2024)	L shaped Photonic Crystal waveguide	Germanium	Electric field distribution by Finite Difference Time Domain method	Pressure sensing in wider range (0-10 G) by optimisation of radius in structure

The current research paper stands out as it not only builds upon previous works by addressing their limitations but also extends the analysis to cover a wider pressure range and provide deeper insights into the photonic crystal's behavior under varying pressure conditions. Additionally, the comprehensive discussion on electric field distribution and output power behavior enhances the understanding of the sensing mechanism; it makes this work a significant advancement in pressure sensing using Germanium-based L-shape photonic crystal structures.

5. Significance and limitations of material selection and applicability within 0-10 GPa pressure range

The significance and limitations of the materials used for pressure sensing, as well as the applicability of the designed structure within the 0-10 GPa pressure range, it can be explained as follows:

5.1. Significance of materials used

Germanium-based materials are chosen for their unique optical and mechanical properties, making them suitable for photonic applications. Germanium offers a high refractive index, which enables efficient light confinement and manipulation within the photonic crystal structure. Additionally, Germanium exhibits nonlinear optical properties, enhancing its sensitivity to external stimuli such as pressure variations. The use of photonic crystals allows for precise control over the propagation of light, enabling the design of highly sensitive and selective sensors.

5.2. Limitations of materials used

Despite its advantages, Germanium also has limitations that need to be considered. One such limitation is its susceptibility to mechanical stress and strain. Excessive pressure may induce mechanical deformation in the Germanium-based photonic crystal structure, leading to changes in its optical properties and sensor performance. Furthermore, Germanium-based materials may have limitations in terms of fabrication complexity and cost, which could impact scalability and practical implementation.

5.3. Applicability within 0-10 GPa pressure range

The designed structure is applicable within the 0-10 GPa pressure range due to the material properties and structural design. Germanium-based photonic crystals are capable of detecting pressure variations within this range with high sensitivity and accuracy. Beyond this pressure range, the mechanical stress on the photonic crystal structure may exceed the material's limits, leading to

performance degradation or structural failure. Therefore, the chosen pressure range aligns with the material's capabilities and ensures reliable sensor operation while maximizing sensitivity and dynamic range. Germanium-based photonic crystals offer significant advantages for pressure sensing applications, it is essential to acknowledge their limitations and design sensors within the appropriate pressure range to ensure optimal performance and reliability.

6. Conclusion

To conclude, we have systematically examined the L shape bend photonic crystal waveguide at wavelength 1550 nm as well as the applied pressure range, which identifies as a pressure sensor as it increases the signal power with an increment of pressure linearly. The Finite-Difference Time-Domain (FDTD) method is crucial for analyzing the electric field distribution along the defect region in the proposed structure. This computational electromagnetics technique discretizes space into a grid and advances electromagnetic fields in time steps, allowing for the simulation of wave propagation and interactions with structures. In the context of photonic crystal or waveguide configurations, FDTD enables a comprehensive understanding of how the electric field is distributed within the defect region. This insight is essential for optimizing device performance as it directly influences phenomena such as light confinement, scattering, and mode coupling. By running FDTD simulations, researchers can visualize and analyze the spatial variation of electric field intensity, identify regions of high field confinement or leakage, and understand the impact of structural parameters on the field distribution. Ultimately, leveraging the FDTD method provides valuable insights into the behavior of electric fields within the proposed structure, aiding in the design and optimization of photonic devices for applications such as sensing, communication, and optical signal processing. The simulation upshot affirmed that nonlinear and linear power increment with respect to pressure at different germanium rods, which performs as an optical pressure sensor. We observed that it is the right candidate for a radius of 430 nm due to the linear behavior and another application is that power amplification occurs at a radius of 440 nm. Therefore, our proposed structure can draw scientist's interest in producing the same due to its prospective purpose as a pressure sensor.

References

[1] J. E. Yablonovitch, Physical Review Letters **58**, 2059 (1987).
[2] S. John, Phys. Rev. Lett. **58**, 2486 (1987).
[3] J. D. Joannopoulos, S.G. Johnson, J. N. Winn, Robort D. Meade, Photonic crystals: Molding the flow of light, 2nd Edn. USA: Princeton University Press (2008).
[4] I. A. Sukhoivanov, I. V. Guryev, Physics and Practical Modeling: Photonic Crystals, Germany, Springer, Heidelberg (2009).
[5] C. S. Mishra, G. Palai, Optik **137**, 37 (2017).
[6] M. M. Hailiang, C. Shuguang, L. X Jing, W. Zhang, Y. Liu, E. Zhu, Optik **179**, 665 (2019).
[7] C. S. Mishra, Anand Nayyar, G. Suseendran, G. Palai, Optik **178**, 509 (2019).
[8] Sangram Kishore Mohanty, G. Palai, Urmilla Bhanja, C. S Mishra, Optik **172**, 861 (2018).
[9] C. S. Mishra, G. Palai, Deo Prakash, K. D. Verma, S. K. Tripathy, Optik **144**, 522 (2017).
[10] C. S. Mishra, M. R. Nayak, S. K. Sahu, G. Palai, Optoelectron. Adv. Mat. **15**(9-10), 420-426 (2021).
[11] A. Lavin, R. Casque, INNBIOD (REF:IPT-2011-1429-010000, (2011) under the Spanish Ministry of Economy and Competitiveness.
[12] C. Y. Chao, L. J. Guo, Journal of Lightwave Technology **24**, 1395 (2006).
[13] Krishnan Vijaya Shanthi, Savarimuthu Robinson, Photonic Sensors **4**(3), 248 (2014).
[14] X. Xiong, P. Lu, D. Liu, Optoelectronics **2**, 219 (2009).
[15] Y. Lu, A. Lal, IEEE 24th International Conference on Micro Electro Mechanical Systems (MEMS), Cancun, 621 (2011).
[16] M. R. Lee, P. M. Fauchet, Optics Letters **32**, 3284 (2007).
[17] H. Kurt, D. S. Citrin, Conference on Lasers and Electro-Optics (CLEO), Atlanta, USA, May 22–27, (2005).
[18] S. C. Buswell, V. A. Wright, J. M. Buriak, V. Van, S. Evoy, Optics Express **16**, 15949 (2007).
[19] M. R. Lee, P. M. Fauchet, Optics Express **15**, 4530 (2007).
[20] S. Mandal, J. Goddard, D. Erickson, Conference on Laser and Electro-Optics/ Conference on Quantum Electronics and Laser Science (CLEO/QELS), San Jose, 1 (2008).
[21] O. Saeed, D. A. Asghar, Photonic Sensors **2**, 92 (2012).
[22] C. S. Mishra, Anand Nayyar, Sandeep Kumar, Bandana Mahapatra, G. Palai, Optik **176**, 56 (2019).
[23] F. Hsiao, C Lee, IEEE Sensors **10**, 1185 (2010).
[24] B. Li, C. Lee, Procedia Engineering **5**, 1418 (2010).
[25] T. Dharchana, A. Sivanantharaja, S. Selvendran, Advances in Natural and Applied Sciences **11**, 26 (2017).
[26] S. Upadhyay, V. L. Kalyani, International Conference ICT4SD, 269 (2016).
[27] Y. Calahorra, A. Husmann, A. Bourdelain, W. Kim, J. Vukajlovic-Plestina, C. Boughey, Q. Jing, A. Fontcuberta i Morral, S. Kar-Narayan, Journal of Physics D: Applied Physics **52**(29), 294002 (2019).
[28] Y. Wang, Aref Bakhtazad, Jayshri Sabarinathan, Proc. SPIE **8007**, 276 (2011).
[29] Aref Bakhtazad, Jayshri Sabarinathan, L. Jeffrey Hutter, 2010 International Symposium on Optomechatronic Technologies, 1-5 (2010).
[30] A. R. Goni, K. Syassen, M. Cardona, Physical Review B **41**, 10104 (1989).

[31] Shangbin Tao, Deyuan Chen, Juebin Wang, Jing Qiao, Yali Duan, Photonic Sensors **6**, 137 (2016).
[32] T. Zouache, A. Hocini, A. Harhouz, R. Mokhtari, Acta Physica Polonica A **131**, 68 (2017).
[33] C. S. Mishra, R. Arunachalam, C. Nayak, M. R. Nayak, S. K. Sahu, G. Palai, Silicon **14**, 4509 (2022).
[34] C. S. Mishra, S. R. Mondal, R. Arunachalam, M. R. Nayak, S. K. Tripathy, G. Palai, Optical and Quantum Electronics **55**(1), 1 (2023).
[35] C. S. Mishra, Optical Material **127**,112298 (2022).
[36] C. S. Mishra, M. R. Nayak, S. K. Tripathy, R. N. Satpathy, G. Palai, J. Optoelectron. Adv. M. **25**(11-12), 521 (2023).
[37] N. Ayyanar, D. Vigneswaran, M. Sharma, M. Sumathi, M. M. Rajan, S. Konar, IEEE Sensors Journal **17**(3), 650 (2016).
[38] M. Turduev, I. H. Giden, C. Babayiğit, Z. Hayran, E. Bor, Ç. Boztuğ, H. Kurt, K. Staliunas, Sensors and Actuators B: Chemical **245**, 765 (2017).
[39] S. Dinodiya, A. Bhargava, Silicon **14**(9), 4611 (2022).
[40] N. C. Panoiu, J. F. McMillan, C. W. Wong, IEEE Journal of Selected Topics in Quantum Electronics **16**(1), 257 (2010).
[41] D. Marris-Morini, Vladyslav Vakarin, Juan Manel Ramirez, Qiankun Liu, Andrea Ballabio, Jacopo Frigerio, Miguel Montesinos, Carlos Alonso-Ramos, Xavier Le Roux, Samuel Serna, Daniel Benedikovic, Daniel Chrastina, Laurent Vivien, Giovanni Isella, Nanophotonics **7**(11), 1781 (2018).
[42] C. S. Mishra, S. Das, M. R. Nayak, P. D. Pukhrambam, A. Panda, G. Palai, Lasers in Engineering **53**(1-2), 105 (2022).
[43] S. Singh, K. Singh, Optik **145**, 495 (2017).
[44] Z. Yu, S. Fan, Advanced Optical Materials **1**(1), 76 (2013).
[45] Bibhatsu Kuiri, Aloke Kumar Pathak, Amlan Das, Binoy Das, Vigneswaran Dhasarathan, Ardhendu Sekhar Patra, Results in Physics **60**, 107639 (2024).
[46] J. Xia, Q. Qiao, G. Zhou, F. S. Chau, G. Zhou, Applied Sciences **10**(20), 7080 (2020).
[47] M. Li, W. P. Huang, Optics Express **26**(20), 25667 (2018).
[48] J. Zhang, Y. Zhao, Y. Ge, M. Li, L. Yang, X. Mao, Micromachines **7**(10), 187 (2016).
[49] M. K. Chhipa, B. T. P. Madhav, B. Suthar, V. Janyani, Photon Network Communications **44**, 30 (2022)
[50] U. Biswas, J.K. Rakshit, B. Suthar, D. Kumar, C. Nayak, International Journal of Numerical Modelling: Electronic Networks, Devices and Fields **35**(2), e2962 (2022).
[51] M. K. Chhipa, B. T. P. Madhav, S. Robinson, V. Janyani, B. Suthar, Optical Engineering **60**(7), 075104 (2021).
[52] U. Biswas, J. K. Rakshit, J. Das, G. K. Bharti, B. Suthar, A. Amphawan, M. Najjar, Silicon **13**, 885 (2021).
[53] M. K. Chhipa, B. T. P. Madhav, B. Suthar, Journal of Computational Electronics **20**, 419 (2021).
[54] Z. Gharsallah, M. Najjar, B. Suthar, V. Janyani, Optical and Quantum Electronics **51**, 1 (2019).
[55] M. Radhouene M. Najjar, M. K. Chhipa, S. Robinson, B. Suthar, Optik **172**, 924 (2018).
[56] E. H. Shaik, N. Rangaswamy, Journal of Modern Optics **63**(10), 941 (2016).
[57] E. H. Shaik, N. Rangaswamy, Optical and Quantum Electronics **48**, 1 (2016).
[58] A. Askarian, F. Parandin, Journal of Computational Electronics **22**(1), 288 (2023).
[59] A. Bhavana, P. D. Pukhrambam, A. Panda, M. G. Daher, International Conference on Micro/Nanoelectronics Devices, Circuits and Systems, Singapore, Springer Nature Singapore, 45 (2023).
[60] T. Li, L. Li, W. Song, G. Zhang, Y. Li, ECS Transactions **58**(40), 65 (2014).
[61] Taehwan Kim, Pavan Bhargava, Christopher V. Poulton, Jelena Notaros, Ami Yaacobi, Erman Timurdogan, Christopher Baiocco, N. Fahrenkopf, S. Kruger, T. Ngai, Y. Timalsina, IEEE Journal of Solid-State Circuits **54**(11), 3061 (2019).
[62] K. Latha, R. Arunkumar, S. Robinson, i-manager's Journal on Digital Signal Processing **7**(1), 12 (2019).

*Corresponding author: gpalai28@gmail.com